X-ray magnetic circular dichroism investigation of spin and orbital moments in Cr_8 and Cr_7Ni antiferromagnetic rings

V. Corradini,[1,*] F. Moro,[1] R. Biagi,[1] U. del Pennino,[1] V. De Renzi,[1] S. Carretta,[2] P. Santini,[2] M. Affronte,[1] J. C. Cezar,[3] G. Timco,[4] and R. E. P. Winpenny[4]

[1]*INFM-CNR S3 National Research Centre and Dipartimento di Fisica, Università di Modena e Reggio Emilia, via G. Campi 213/A, 41100 Modena, Italy*

[2]*Department of Physics, University of Parma, via G. P. Usberti, I-43100 Parma, Italy*

[3]*European Synchrotron Radiation Facility, Boîte Postale 220, F-38043 Grenoble Cédex, France*

[4]*School of Chemistry, University of Manchester, Oxford Road, Manchester M13 9PL, United Kingdom*

(Received 3 August 2007; revised manuscript received 16 October 2007; published 2 January 2008)

We investigated the electronic and magnetic properties of thick films of molecular $\{Cr_8\}$ and $\{Cr_7Ni\}$ antiferromagnetic rings by means of x-ray absorption spectroscopy and x-ray magnetic circular dichroism (XMCD). We determined the local symmetries, the electronic configuration, and the values of orbital and spin moments at the Cr and Ni sites of the molecular rings. XMCD measurements show that the correlation between the Cr and Ni spins in the $\{Cr_7Ni\}$ molecular ring switches from antiferromagnetic to ferromagnetic with increasing temperature. Experimental data are interpreted using XMCD sum rules that allow the separate evaluation of the spin and the orbital contributions to the total magnetic moment of the ring as a function of temperature and magnetic field. The magnetic behaviors experimentally observed are compared with the results of spin-Hamiltonian calculations, based on microscopic parameters derived by inelastic-neutron scattering and low-temperature specific-heat measurements. The very good agreement between experimental data and calculations is a clear indication of the integrity of molecules. The temperature dependence of the ion magnetic moments results from the interplay between Zeeman and isotropic-exchange contributions, and is well captured by the theoretical model.

DOI: 10.1103/PhysRevB.77.014402 PACS number(s): 75.50.Xx, 33.55.+b, 78.70.Dm, 75.10.Dg

INTRODUCTION

Considerable interest and experimental works have been recently devoted to control the deposition of molecular nanomagnets (MNMs) on surfaces. All these efforts will eventually allow the exploitation of the functionalities of nanomagnets at molecular level. One of the still-open issues is, however, the magnetic characterization of these layered systems. Indeed, the experimental determination of the magnetic properties of MNM layers is very challenging and, as a matter of fact, the fundamental issue of their possible modifications due to interaction with the surface is still unexplored. Among the large family of MNMs, heterometallic $\{Cr_7Ni\}$ rings are a new class of molecules on which quantum phenomena at macroscopic scale have been observed,[1,2] and they were also recently proposed as molecular hardware to encode *qubits*.[3–9] They are antiferromagnetically coupled cyclic systems containing seven Cr^{3+} (spin $s=3/2$) ions and one Ni^{2+} ion ($s=1$).[10–12] The ground $S=1/2$ doublet of the ring is energetically well separated from the first excited triplet: at zero magnetic field, $\Delta_0/k_B=13$ K.[5,13] The precursor of this family of MNMs is a molecular ring containing eight antiferromagnetically coupled Cr^{3+} ions disposed in an octagonal geometry, having an $S=0$ ground state and chemical formula $[Cr_8F_8(O_2C^tBu)_{16}]$.[10,14] In order to fully exploit the potentialities of such molecular antiferromagnetic (AF) rings in nanoelectronics, the design of appropriate derivatives and the implementation of procedures to graft them onto suitable surfaces are crucial. We have recently reported the synthesis of $\{Cr_7Ni\}$ sulphur-functionalized derivatives and an effective procedure to obtain a single-layer distribution of Cr_7Ni rings grafted on Au(111).[6,12,15] These are basic steps for the fabrication of arrays of single-addressable MNMs, and work is in progress to measure the properties of these layers.

Due to its high sensitivity and its chemical selectivity, x-ray magnetic circular dichroism (XMCD) is a powerful technique to measure the magnetic properties of thin layers. Yet, to the best of our knowledge, only a few works have been published so far on XMCD characterization of single molecule nanomagnets[16–19] and none on single-layer MNMs due to several experimental difficulties. The usual XMCD analysis is based on the exploitation of the so-called sum rules, which, in principle, enable the element- and shell-specific measurement of the orbital and of the spin moments separately. Yet, the effective application of these rules faces several drawbacks, which we briefly mention here and fully discuss afterwards: the non-negligible presence of the magnetic dipole term, the evaluation of the correct number of $3d$ holes, and the problem of the j-j mixing effect.[20,21] Therefore, in order to verify the applicability of sum rules to MNMs, it is important to test them on benchmark samples and to compare with theoretical results. For this reason, we decided to study bulklike samples in the form of polycrystalline thick films of MNMs obtained by drop casting before moving to single molecular layers.

In this paper, we report on a joint experimental and theoretical investigation on the electronic and magnetic properties of thick films (TFs) of two MNMs, namely, $[Cr_8F_8Piv_{16}]$ (where $Piv=O_2CC(CH_3)_3$; referred to as Cr_8-piv in the following[14]) and $[Me_2NH_2][Cr_7NiF_8Piv_{16}]$ (referred to as Cr_7Ni-piv in the following[11]) AF rings obtained by drop casting. These systems were studied by means of

 ©2008 The American Physical Society

x-ray absorption spectroscopy (XAS) and XMCD techniques, and results are compared with spin-Hamiltonian calculations. The Cr_8-piv ring was studied as a benchmark in order to fix the best parameters for the application of the sum rules to the Cr^{3+} ions. This allows us to properly deal with the more interesting Cr_7Ni-piv system, verifying the applicability of sum rules to this system and finding the best parameters for the Ni^{2+} ion. The total magnetic moments experimentally derived for Cr and Ni ions are in excellent agreement with spin-Hamiltonian calculations based on models previously fitted to inelastic neutron scattering (INS) and specific-heat data.[13,22,23] In particular, the observed reversal of the Ni magnetic moment with increasing T is correctly predicted and explained within our model, in terms of the interplay between Zeeman and isotropic-exchange Hamiltonian contributions. In the next section, we describe the experimental details, while results and discussion are reported in the following section.

EXPERIMENT

The XAS-XMCD experiments were carried out at the ID8 beamline of the European Synchrotron Radiation Facility (ESRF) in Grenoble (France). The photon source was an Apple II undulator that delivers a high flux (10^{13} photons/s) of polarized light. However, in order to avoid sample degradation induced by radiation exposure, measurements have been done with a beam flux attenuated by more than 1 order of magnitude. Integrity checks based on XAS spectra have been performed throughout the experiment, never finding any trace of degradation.

The XMCD measurements at the Cr and Ni $L_{2,3}$ edges were performed in total electron yield mode using circularly polarized light with about 100% polarization rate with an external magnetic field up to 5 T. In our experiment, the direction of the impinging beam is parallel to the applied magnetic field (**H**) and both are perpendicular to the sample surface (along the z axis). The dichroic spectrum is the difference between the XAS spectra taken with the helicity of the incident photon (**P**) parallel ($\sigma^{\uparrow\uparrow}$) and antiparallel ($\sigma^{\uparrow\downarrow}$) to the sample magnetization (**M**). In our experiment, in order to minimize the effects of field inhomogeneity, we first fixed the field and switched the polarization parallel and antiparallel, then made the same with opposite field direction.[24] The $\sigma^{\uparrow\uparrow}$ ($\sigma^{\uparrow\downarrow}$) absorption spectra are the mean value of the spectra collected with the helicity parallel (antiparallel) to the sample magnetization.

The lowest sample temperature reached was about 10 K and the base pressure of the experimental chamber was 1.0×10^{-10} mbar. The samples investigated are drop-casted TFs obtained by liquid phase deposition from a saturated solution of the Cr_8-piv (Ref. 14) and Cr_7Ni-piv (Ref. 11) molecular rings on a highly ordered pyrolytic graphite substrate. We expect no significant contribution from the substrate, since the thickness of deposited multilayer is much higher than the sampling depth of the XMCD technique.

RESULTS AND DISCUSSION

As a preliminary investigation, we characterized the Cr_8-piv and Cr_7Ni-piv drop-casted TFs by means of x-ray photoelectron spectroscopy (XPS) *on campus*. The XPS analysis (spectra not reported here) indicated that the ring stoichiometry of the core is preserved in the drop-casting procedure, since the ratios between the normalized core level intensities are close to the expected stoichiometric values.

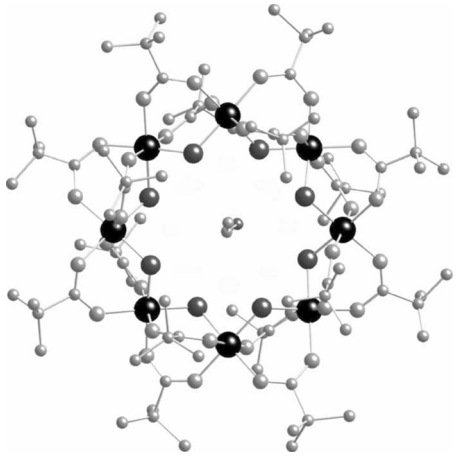

FIG. 1. The structure of $[Me_2NH_2][Cr_7NiF_8(O_2CCMe_3)_{16}]$ (Top view). The large dark circles represent the Cr/Ni disordered atoms within the wheel, the small dark circles indicate the F, and the large and small gray circles are the O and C atoms, respectively. H atoms are omitted for clarity.

The structure of the heterometallic Cr_7Ni-piv ring,[14] displayed in Fig. 1, is very similar to that of the neutral Cr_8-piv.[11] Each Cr-Cr (Cr-Ni) vector is bridged by a μ-fluoride bridge and two 1,3-bridging pivalates. The local symmetry of each chromium or nickel is represented by an octahedron with six apical atoms: four O atoms (Cr-O $=1.95\pm0.01$ Å) and two F atoms (Cr-F$=1.93\pm0.01$ Å), at the center of which lies the metal ion in a slightly distorted octahedral environment. Due to the incomplete equivalence between F and O, the symmetry of the coordination around each ion is actually C_2 and not C_3. However, the very similar bond lengths and angles around the magnetic ion leads to an almost perfect equivalence between F and O, as also evidenced by *ab initio* calculations performed on Cr_8 and Cr_4Ni_4 AF rings[25,26] by density-functional theory methods, which allow the assumption of a nearly pure triaxial symmetry (C_3) for Cr and Ni ions.

The oxidation states, the local symmetries, and the spin and orbital magnetic moments of the Cr and Ni ions in both rings were investigated by means of XAS and XMCD. Indeed, it is well known that the details of XAS line shape are very sensitive to the electronic and symmetry properties of the investigated systems. A direct comparison with the absorption spectra of well-defined Cr-based and Ni-based compounds can, therefore, provide clear clues on the valence and the geometrical environment of each magnetic ion. In Fig. 2, left panel, the Cr $L_{2,3}$ XAS and XMCD spectra measured for Cr_8-piv and Cr_7Ni-piv are compared with metallic Cr,[27] CrO_2 (Cr^{4+} oxidation state and C_4 symmetry),[28] and Cr_2O_3 (Cr^{3+} oxidation and C_3 symmetry).[29] Since the α-Cr_2O_3 compound is AF and thus not dichroic, comparison with the XMCD signal of the $Cr_{0.07}Al_{1.93}O_3$,[29] where chromium presents the

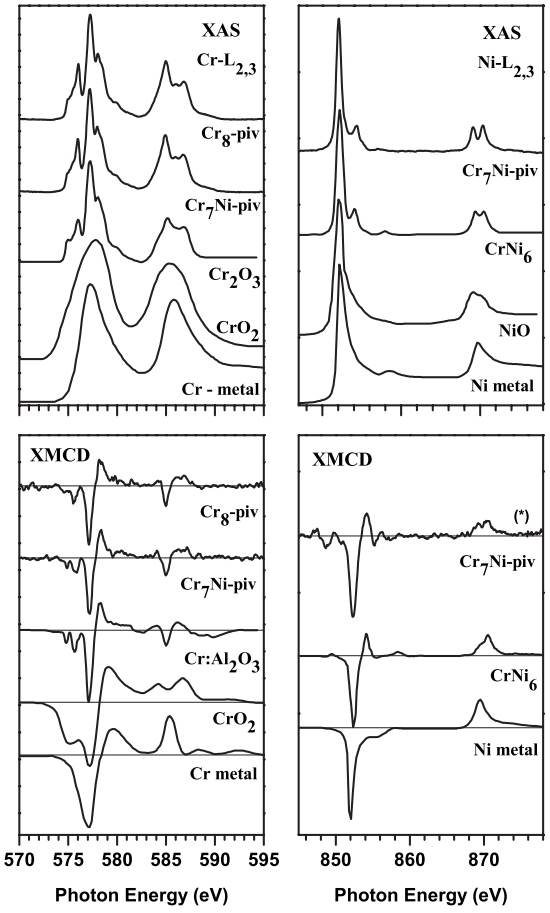

FIG. 2. (Left panel) The Cr $L_{2,3}$ XAS and XMCD spectra for Cr_8-piv and Cr_7Ni-piv, taken at 10 K and 5 T, compared with metallic Cr (Ref. 27), CrO_2 (Ref. 28), and Cr_2O_3 (Ref. 29). (Right panel) The Ni $L_{2,3}$ XAS and XMCD signals for Cr_7Ni-piv, taken at 10 K and 5 T, compared with metallic Ni (Ref. 30), NiO (Ref. 31), and $CrNi_6$ (Ref. 16). (*) The Cr_7Ni-piv dichroic spectrum has been reversed in order to facilitate the comparison with the line shape of the other spectra.

same C_3 local symmetry, was considered. The Cr_8-piv at 0 K is expected to have no dichroic signal since its ground state is a nonmagnetic singlet, as experimentally and theoretically proven.[13,14] On the other hand, in presence of a magnetic field, an increment of the temperature produces an increase of the magnetic moment entirely due to thermally populated excited states ($S=1,2,3,\ldots$).[13,22] In both Cr_8-piv and Cr_7Ni-piv (Fig. 2, left panel), the Cr $L_{2,3}$ XAS and XMCD spectra present the same profile of the α-Cr_2O_3 XAS and of the $Cr_{0.07}Al_{1.93}O_3$ XMCD.[29] In the spectral line shape eight similar features can be identified, which are the direct fingerprint of the presence of Cr^{3+} in an octahedral environment, as indicated in Ref. 29 Moreover, the Cr_8-piv and Cr_7Ni-piv XMCD spectra at the L_2 edge are partially above and partially below the zero axis, like in the α-Cr_2O_3 case, while they are completely positive in CrO_2 and Cr-metallic systems. In Fig. 2, right panel, the Ni $L_{2,3}$ XAS and XMCD signals measured for Cr_7Ni-piv are compared with metallic Ni,[30] NiO (Ni^{2+} oxidation state and C_4 symmetry),[31] and $CrNi_6$ clusters (Ni^{2+} oxidation state and C_3 symmetry).[16] The

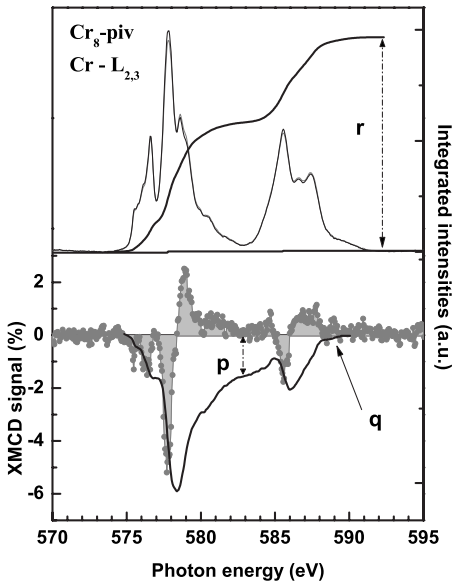

FIG. 3. (Upper panel) Cr $L_{2,3}$ XAS spectra taken with $\sigma^{\uparrow\uparrow}$ and $\sigma^{\uparrow\downarrow}$ circularly polarized light for Cr_8-piv TF at 5 T and 10 K. (Lower panel) XMCD spectrum (dotted line) and its integral (continuous line). The parameters p, q, and r are the values of the three integrals needed for the sum-rules analysis.

Ni XMCD signal in NiO is zero. The Ni XAS and XMCD spectra of Cr_7Ni-piv present the same line shape of the $CrNi_6$ system, which is characterized by Ni^{2+} in octahedral symmetry.[16] Indeed, the two peaks at the L_3 edge and a partially resolved doublet structure at the L_2 edge are both characteristic of a high-spin (triplet state) Ni^{2+} ion in octahedral environment.[32,33]

Information on the nature of the exchange interactions can be deduced from the sign of the XMCD signal.[16,34] In Figs. 3 and 4 are reported the Cr $L_{2,3}$ absorption spectra taken with $\sigma^{\uparrow\uparrow}$ and $\sigma^{\uparrow\downarrow}$ circularly polarized light (upper panel), the dichroic signal and its integral (lower panel) for Cr_8-piv and Cr_7Ni-piv, respectively, measured at 10 K with an external magnetic field (**H**) of 5 T. In Fig. 5, the Ni $L_{2,3}$ absorption spectra of Cr_7Ni-piv [Fig. 5(a), upper panel] and the dichroic signal measured at 10 K [Fig. 5(a), lower panel] and at 25 K [Fig. 5(b)] are reported. The negative XMCD signal at the Cr L_3 edge and the positive one at the L_2 edge prove that, for all T and **H**, the Cr total magnetic moment in both Cr_8-piv and Cr_7Ni-piv rings is parallel to **H**. In the case of Ni in the Cr_7Ni-piv at 10 and 15 K on the contrary, we observed [Fig. 5(a)] a positive XMCD signal at the L_3 edge and a negative one at the L_2 edge, demonstrating that the Ni total magnetic moment is antiparallel to **H**, as expected. This result is a direct proof of the local AF coupling between Cr and Ni in the Cr_7Ni-piv ring at low temperatures (up to about 15 K). However, most interestingly, the Ni-Cr correlation changes by increasing temperature, as clearly shown in Fig. 5(b); at 25 K, an inversion of the sign of Ni dichroism occurs, indicating the change to a ferromagnetic correlation.

In order to quantitatively compare these results with theoretical calculations, we analyzed the data by applying the so-called spin and orbital moment sum rules.[35–38] Indeed,

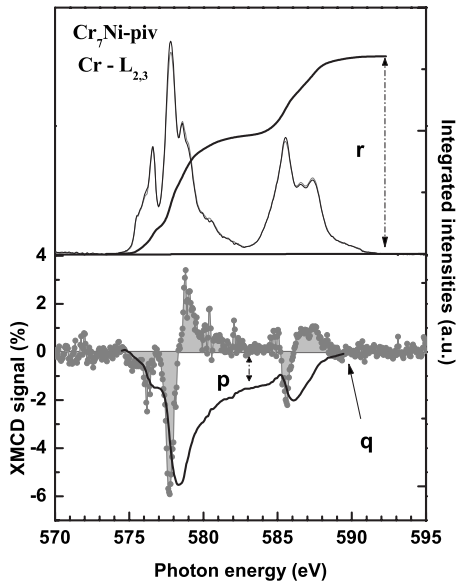

FIG. 4. (Upper panel) Cr $L_{2,3}$ XAS spectra taken with $\sigma^{\uparrow\uparrow}$ and $\sigma^{\uparrow\downarrow}$ circularly polarized light for Cr_7Ni-piv TF at 5 T and 10 K. (Lower panel) XMCD spectrum (dotted line) and its integral (continuous line). The parameters p, q, and r are the values of the three integrals needed for the sum-rules analysis.

from the experimental spectra, it is possible to extract the spin (m_s) and orbital (m_o) magnetic moments carried by the Cr^{3+} and Ni^{2+} ions by using simple relations between the intensities of the dichroic signals at the L_3 (A) and L_2 (B) edges, provided by the spin and orbital moment sum rules:[35–38] $[A-2B] \propto (m_s + m_D^{\alpha})$, $[A+B] \propto m_o^{\alpha}$, where α specifies the photon direction **P** with respect to the applied field **H**, m_D^{α} is the intra-atomic magnetic dipole moment, and m_o^{α} is the orbital moment along the field direction α. These sum rules must be normalized to the white line intensity: $(I_{L3} + I_{L2}) = C(N + N_Q^{\alpha})$, where N represents the isotropic number of $3d$ holes and N_Q^{α} the anisotropic charge density term.[38] In our experimental setup we have selected a photon direction **P** parallel to applied field **H** ($\alpha=0$), both oriented along the z axis.

As mentioned in the Introduction, the quantitative application of these rules faces several drawbacks, which must be carefully considered, namely, (i) the presence in the spin moment sum rule of a term proportional to the magnetic dipole operator (T_z), which is quite troublesome; (ii) the determination of the effective number of $3d$ holes in the ground state; and (iii) the complication deriving from the j-j mixing effect due to the quantum mechanical overlapping of L_2 and L_3 excitations.[20,21] We proceeded as follows:

(i) Since in the Cr_8-piv and Cr_7Ni-piv rings each ion is in a slightly distorted octahedral geometry with an almost triaxial symmetry, the t_{2g} (d_{xy}, d_{xz}, d_{yz}) and e_g ($d_{x_2-y_2}, d_{3z_2-r_2}$) manifolds possess a nearly isotropic charge density.[25,38] Similarly, the spin density and the orbital moment can be safely considered as rather isotropic, thus causing the quadrupole terms m_D^{α} and N_Q^{α} to vanish and allowing the application of the isotropic sum rules.[24,37]

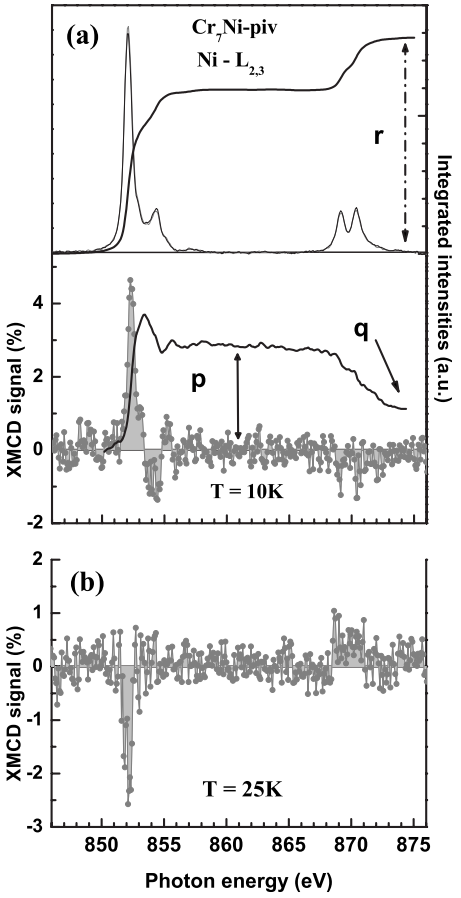

FIG. 5. (a) (Upper panel) Ni $L_{2,3}$ XAS spectra taken with $\sigma^{\uparrow\uparrow}$ and $\sigma^{\uparrow\downarrow}$ circularly polarized light for Cr_7Ni-piv TF at 5 T and 10 K. (Lower panel) XMCD spectrum (dotted line) and its integral (continuous line) at 10 K. (b). XMCD spectrum at 5 T and 25 K. The parameters p, q, and r are the values of the three integrals needed for the sum-rules analysis.

(ii) For the number of $3d$ holes, since we can neglect the anisotropic term, we have directly used the nominal values of $N=7$ for Cr and $N=2$ for Ni.

(iii) The sum rules can be properly applied when the separation between the $2p_{3/2}$ and $2p_{1/2}$ excitations is large enough to clearly distinguish the $j_{3/2}$ and $j_{1/2}$ excitations. If the spectral features of the L_2 and L_3 edges overlap, the absorption process involves a quantum mechanical superposition of $2p_{3/2}$ and $2p_{1/2}$ excitations.[20,21] In order to include this mixing effect, in the case of Cr, the spin moment sum rule must be multiplied by a spin correction (SC) factor, which can be evaluated from the ratio between the intensities of the Cr XAS at the L_2 and L_3 edges.[21] The value we obtained for both the Cr_8-piv and Cr_7Ni-piv systems is 1.75, which is intermediate between the values of SC for a layer of metallic Cr (1.4) and for bulk Cr (2).[21] As shown in the following, the good agreement between experimental and theoretical values of the orbital and spin moments of the studied systems proved the validity of our choice of parameters (number of vacancies and SC factor).

Before applying the XMCD sum rules, we subtracted a two-step-like function from the XAS spectra to remove the

L_3 and L_2 edge jumps.[39] We call r the value of the integral of the whole XAS spectra after the edge-jump removal, which represents the white line intensity $r=(I_{L3}+I_{L2})$. It is useful to introduce a couple of parameters, p and q, which can be obtained directly from the integral of the XMCD spectra, as shown in Figs. 3–5 ($p=A$, $q=A+B$). Thus, the orbital and spin moments can be calculated by the following expressions:[39]

$$\frac{m_S}{\mu_B} = -\frac{(6p-4q)}{r} N_{eff} SC, \quad \frac{m_o}{\mu_B} = -\frac{4q}{3r} N_{eff}.$$

The vanishing of the dichroic signal integral at the Cr $L_{2,3}$ edges ($q=0$) shows the total quenching of the orbital momentum of the Cr^{3+} ions by the crystal field in both Cr_8-piv and Cr_7Ni-piv systems,[39] as expected from thermodynamic and INS measurements. On the contrary, the integral of the Ni dichroic signal does not completely vanish, giving the direct experimental evidence of the only partial quenching of the orbital momentum for the Ni^{2+} ions. The value of the orbital moment derived by the sum rules is about 8%–12% of the spin moment, for all measured temperatures and magnetic fields, in excellent agreement with the value implied by the gyromagnetic factor of Ni ions (see discussion below).

We have derived the mean value of the spin and orbital moments (along the z axis) for each Cr and Ni atom at different magnetic fields (1, 3, 4, and 5 T) and at different temperatures. In order to obtain the total Cr magnetic moment of the ring, the values for the single atom have to be multiplied by the number of Cr atoms in each ring (8 for Cr_8 and 7 for Cr_7Ni). In Figs. 6 and 7, the experimentally derived total magnetic moments have been compared with the results of spin-Hamiltonian calculations for Cr_8-piv and Cr_7Ni-piv, respectively.

By labeling z' the direction of the ring axis, the microscopic spin Hamiltonian has the form

$$H = \sum_i J_{i,i+1} \mathbf{s}_i \cdot \mathbf{s}_{i+1} + \sum_i d_i [s_{z',i}^2 - s_i(s_i+1)/3] + \sum_{ij} \mathbf{s}_i \cdot \mathbf{D}_{ij} \cdot \mathbf{s}_j + \mu_B \mathbf{H} \cdot \sum_i \underline{\underline{g}}_i \cdot \mathbf{s}_i,$$

where the first term represents isotropic nearest-neighbor exchange, the second and third terms represent anisotropic interactions (crystal field and anisotropic dipole-dipole coupling), and the last term is the Zeeman coupling to an external field $\mathbf{H}$. The component along $\mathbf{H}$ of the total magnetic moment (spin plus orbital moment) of each ion can be numerically determined once the microscopic parameters are fixed. These parameters, reported in the caption of Fig. 8, have been directly determined by fitting INS and low-temperature specific-heat data.[13,22,23] A spherical average has been performed to simulate experimental data. Convergence of thermal averages requires including energy levels up to about $5k_BT$, which corresponds to hundreds of levels at 25 K (see Fig. 8). The gyromagnetic factor of Cr ions ($g_{Cr}=1.98$) is very close to the spin-only value of 2, indicating that the Cr magnetic moment is almost entirely due to spin, whereas the Ni factor $g_{Ni}=2.2$ is indicative of an orbital contribution of 10% of the spin one.

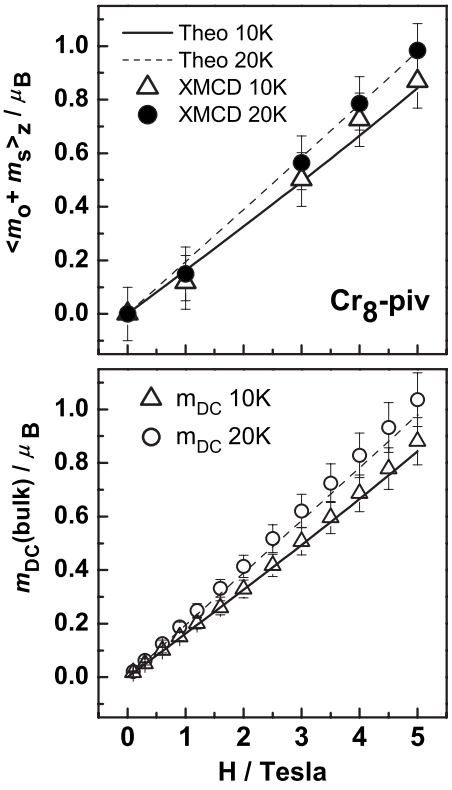

FIG. 6. Total magnetic moment vs applied magnetic field for the Cr_8-piv system at 10 and 20 K: spin-Hamiltonian calculations (upper panel) compared with the mean value along the z axis of the Cr total magnetic moment derived from the XMCD sum rules and (lower panel) compared with bulklike magnetization measured on polycrystalline sample.

The behavior of the magnetic moments as a function of field and temperature, displayed in Fig. 6, upper panel, and Fig. 7, shows very good quantitative agreement between experiment and theory. In Fig. 6, lower panel, the bulk magnetization measured on a Cr_8 polycrystalline sample is also reported for comparison. Since there are no free parameters in the spin Hamiltonian, this agreement for both Cr_8-piv and Cr_7Ni-piv systems clearly supports our choice for the SC factor=1.75 and the number of holes $N=7$ for chromium. This result shows that the controversial method of experimentally deriving the SC factor from the L_2/L_3 ratios suggested by Goering,[21] though not universally applicable, has proven to be effective at least in our case of Cr^{+3} systems. As shown in Fig. 7, the experimental values of the Ni magnetic moments are slightly smaller than the theoretical prediction. This observation can be explained by taking into account that even in the case of Ni the jj mixing, though much smaller than for Cr, is not completely negligible and, therefore, a small correction factor may have to be introduced. This fact is supported by theoretical calculations based on different approaches, which estimated a SC=1.1 for a Ni^{2+} in C_3 symmetry.[20,40] As this would in any case provide only a minor correction, for sake of simplicity, we decided to omit this further parameter from our analysis. The theoretical model provides important clues to understand the observed behaviors since the temperature dependence of the local magnetic

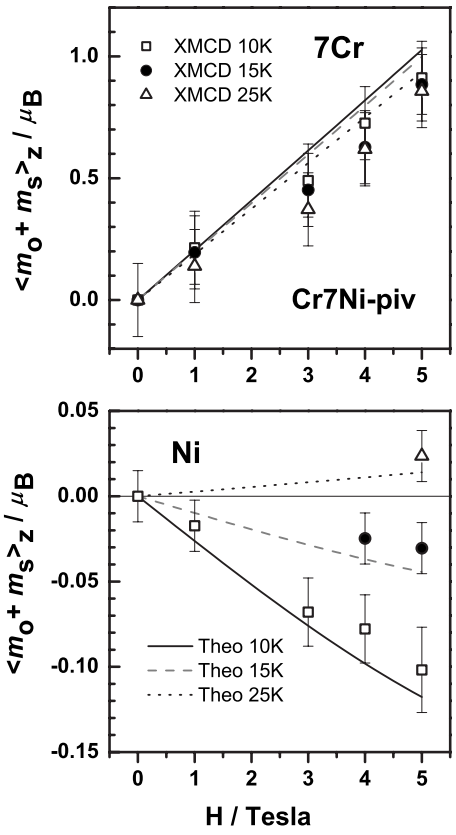

FIG. 7. Cr (upper panel) and Ni (lower panel) total magnetic moments experimentally derived from the XMCD sum rules vs applied magnetic field at 10, 15, and 25 K (symbols) compared with the results of spin-Hamiltonian calculations for the Cr_7Ni-piv system (continuous lines). The magnetic moment uncertainty takes into account the signal to noise ratio of the spectrum it was derived from.

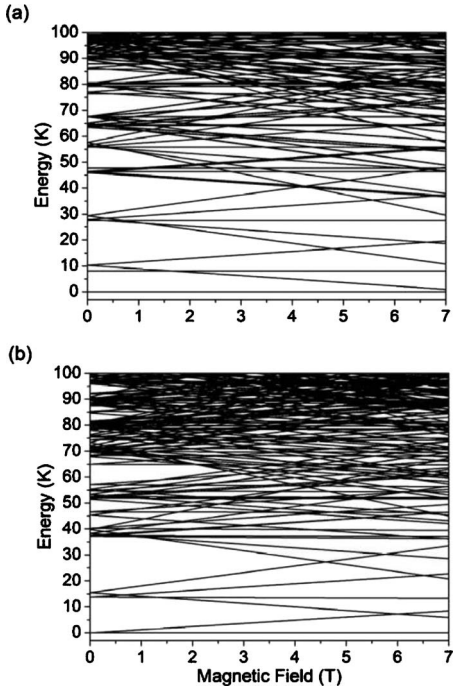

FIG. 8. Calculated field dependence of the low-lying energy levels of (a) Cr_8 and (b) Cr_7Ni-piv relative to the ground-state energy. The magnetic field is set parallel to the ring axis. Parameters used in calculations are $J_{Cr\text{-}Cr}=17$ K, $d_i=-0.34$ K for Cr_8, and $J_{Cr\text{-}Cr}=17$ K, $J_{Cr\text{-}Ni}=19.6$ K, $d_{Cr}=-0.34$ K, and $d_{Cr}=-4$ K for Cr_7Ni.

moments reflects the structure of the low-lying levels of the molecular Hamiltonian. In the experimental T range, the populated levels are hundreds (see Fig. 8), hence the resulting behavior is nontrivial. Though the two systems studied are very similar AF rings, their spectral properties are very different because the presence of Ni changes both the topology of the chain and the total-spin quantum numbers. In particular, in Cr_8-piv all spins are equivalent and each average local magnetic moment is equal to $1/8$ of the static magnetization M of the system (see Fig. 6) and is parallel to the applied field. On the contrary, in Cr_7Ni-piv, the magnetic field produces a nonuniform and alternate in sign pattern of local moments which are not proportional to M. The only constraint is that the sum of all local moments is equal to M. For instance, the calculated Cr_7Ni-piv magnetic moments at 5 T and 10 K are (in μ_B units): 0.37, −0.13, 0.32, −0.1, 0.32, −0.13 and 0.37 for the seven Cr ions and −0.12 for the Ni ion, giving a total magnetization of the ring $M=0.9\mu_B$. Thus, the average of the absolute values of the Cr moments ($0.25\mu_B$) is about twice the Ni moment, while the average of the Cr moments (taking into account the sign of each moment) is $0.146\mu_B$ which is the value considered for the comparison with the XMCD sum rules in Fig. 7.

Since the Cr_8-piv ground state is a nonmagnetic singlet, it does not contribute to the magnetic moment which, therefore, entirely comes from thermally populated excited states. Thus, in presence of a magnetic field, increasing T from zero produces a growing moment (see Fig. 6). In the case of Cr_7Ni-piv, the ground state is a magnetic $S=1/2$ doublet and the T dependence of the Cr and Ni magnetic moments is determined by the balance of the different contributions from the ground and excited manifolds. For instance, when T varies from 10 K to 15 and 25 K, the sum of the seven Cr moments decreases, whereas at low T, the Ni moment is antiparallel to the external field, while by increasing T (see, e.g., the 25 K curve), it smoothly reverts passing through zero and becomes parallel to the applied field (see Fig. 7). This behavior can be explained in terms of the interplay between Zeeman and isotropic-exchange contributions. As long as the Zeeman energy is much smaller than isotropic exchange, the latter favors in the lowest-lying eigenstates a staggered pattern of local magnetic moments. Thus, at low T (e.g., 10 K), the average Ni moment is opposite to the total average Cr moment. With the Ni spin smaller than the Cr one, the field then selects the staggered configuration with the total Cr moment parallel to **H** (and the Ni moment antiparallel) in order to minimize the Zeeman energy. By increasing T, the Ni average moment smoothly reverts passing through zero and becomes parallel to the applied field and to the total Cr moment. This change of sign occurs because of the thermal population of excited states (e.g., the $S=3/2$ quartet), in which the staggered pattern of local moments is

partially broken. Eventually, in high-energy multiplets, the pattern is completely destroyed because in these multiplets correlations tend to become ferromagnetic. Thus, on increasing T, the average Ni moment is no longer constrained to be opposite to the total average Cr moment.

While in the total Cr moment fine details are partially washed out by the sum of eight or seven ions, the behavior of the Ni moment provides a more sensitive probe of the molecular eigenstates. The reversal of the Ni moment direction occurs at a given temperature linked to the detail of the exchange interactions, in particular, the ratio of the Cr-Cr to the Cr-Ni exchange constants. The agreement between calculations and experiments gives further support to the ratio determined by INS.[13,23]

CONCLUSIONS

Drop-casted TFs of the prototype Cr_8-piv and Cr_7Ni-piv AF molecular rings have been investigated by XAS and XMCD. The electronic configuration of the molecular rings and the T and **H** dependences of the orbital and spin moments at the Cr and Ni sites have been determined and found to be in very good agreement with spin-Hamiltonian calculations. In particular, the orbital moment is almost completely quenched in Cr ions, whereas in Ni ions, it is clearly not vanishing.

The chemical selectivity of the technique allowed us to directly detect a switching in the Ni magnetization, i.e., the antiferromagnetic correlation between the Cr and Ni spins at low T, and its conversion to a ferromagnetic one with increasing T. This finding is nicely predicted and explained by the model calculations. These results show that XMCD is a very powerful technique for the characterization of the magnetic behaviors of heterometallic MNMs and that sum-rules analysis is applicable for this kind of compounds, giving reliable quantitative values of element-specific spin moments. Hence, thanks to its submonolayer sensitivity, XMCD represents the most suitable technique for the magnetic investigation of a single-layer distribution of MNMs deposited on suitable surfaces, which is the next important step toward technological applications.

ACKNOWLEDGMENTS

We are grateful to G. Amoretti and I. Marri for stimulating and helpful discussions. This work has been carried out within the framework of the EU Network of Excellence "MAGMANet" Contract No. 515767 and supported by the PRIN No. 2006029518 of Italian Ministry of Research and EPSRC (UK).

*valdis@unimore.it

[1] S. Carretta, P. Santini, G. Amoretti, M. Affronte, A. Ghirri, I. Sheikin, S. Piligkos, G. Timco, and R. E. P. Winpenny, Phys. Rev. B **72**, 060403(R) (2005).

[2] S. Carretta, P. Santini, G. Amoretti, T. Guidi, J. R. D. Copley, Y. Qiu, R. Caciuffo, G. Timco, and R. E. P. Winpenny, Phys. Rev. Lett. **98**, 167401 (2007).

[3] F. Meier, J. Levy, and D. Loss, Phys. Rev. B **68**, 134417 (2003).

[4] F. Meier, J. Levy, and D. Loss, Phys. Rev. Lett. **90**, 047901 (2003).

[5] F. Troiani, A. Ghirri, M. Affronte, S. Carretta, P. Santini, G. Amoretti, S. Piligkos, G. Timco, and R. E. P. Winpenny, Phys. Rev. Lett. **94**, 207208 (2005).

[6] M. Affronte, F. Troiani, A. Ghirri, A. Candini, M. Evangelisti, V. Corradini, S. Carretta, P. Santini, G. Timco, and R. E. P. Winpenny, J. Phys. D **40**, 2999 (2007).

[7] F. Troiani, M. Affronte, S. Carretta, P. Santini, and G. Amoretti, Phys. Rev. Lett. **94**, 190501 (2005).

[8] A. Ardavan, O. Rival, J. J. L. Morton, S. J. Blundell, A. M. Tyryshkin, G. A. Timco, and R. E. P. Winpenny, Phys. Rev. Lett. **98**, 057201 (2007).

[9] W. Wernsdorfer, Nat. Mater. **6**, 174 (2007).

[10] E. J. L. McInnes, S. Piligkos, G. A. Timco, and R. E. P. Winpenny, Coord. Chem. Rev. **249**, 2577 (2005).

[11] F. K. Larsen, E. J. L. McInnes, H. El Mkami, J. Overgaard, S. Piligkos, G. Rajaraman, E. Rentschler, A. A. Smith, G. M. Smith, V. Boote, M. Jennings, G. A. Timco, and R. E. P. Winpenny, Angew. Chem., Int. Ed. **42**, 101 (2003).

[12] M. Affronte, F. Troiani, A. Ghirri, S. Carretta, P. Santini, V. Corradini, R. Schuecker, C. Muryn, G. Timco, and R. E. P. Winpenny, Dalton Trans. **23**, 2810 (2006).

[13] S. Carretta, J. van Slageren, T. Guidi, E. Liviotti, C. Mondelli, D. Rovai, A. Cornia, A. L. Deardon, F. Carsughi, M. Affronte, C. D. Frost, R. E. P. Winpenny, D. Gatteschi, G. Amoretti, and R. Caciuffo, Phys. Rev. B **67**, 094405 (2003); M. Affronte *et al.*, Eur. Phys. J. B **15**, 633 (2000); Appl. Phys. Lett. **84**, 3468 (2004).

[14] J. van Slageren, R. Sessoli, D. Gatteschi, A. A. Smith, M. Helliwell, R. E. P. Winpenny, A. Cornia, A. Barra, A. G. M. Jensen, E. Rentschler, and G. A. Timco, Chem.-Eur. J. **8**, 277 (2002).

[15] V. Corradini, R. Biagi, U. del Pennino, V. De Renzi, A. Gambardella, M. Affronte, C. A. Muryn, G. A. Timco, and R. E. P. Winpenny, Inorg. Chem. **46**, 4937 (2007).

[16] M.-A. Arrio, A. Scuiller, Ph. Sainctavit, C. Cartier dit Moulin, T. Mallah, and M. Verdaguer, J. Am. Chem. Soc. **121**, 6414 (1999).

[17] H. Wende, M. Bernien, J. Luo, C. Sorg, N. Ponpandian, J. Kurde, J. Miguel, M. Piantek, X. Xu, Ph. Eckhold, W. Kuch, K. Baberschke, P. M. Panchmatia, B. Sanyal, P. M. Oppeneer, and O. Eriksson, Nat. Mater. **6**, 516 (2007).

[18] P. Ghigna, A. Campana, A. Lascialfari, A. Caneschi, D. Gatteschi, A. Tagliaferri, and F. Borgatti, Phys. Rev. B **64**, 132413 (2001).

[19] R. Moroni, C. Cartier dit Moulin, G. Champion, M. A. Arrio, P. Sainctavit, M. Verdaguer, and D. Gatteschi, Phys. Rev. B **68**, 064407 (2003).

[20] J. P. Crocombette, B. T. Thole, and F. Jollet, J. Phys.: Condens. Matter **8**, 4095 (1996).

[21] E. Goering, Philos. Mag. **85**, 2895 (2005), and references therein.

[22] M. Affronte, T. Guidi, R. Caciuffo, S. Carretta, G. Amoretti, J.

Hinderer, I. Sheikin, A. G. M. Jansen, A. A. Smith, R. E. P. Winpenny, J. van Slageren, and D. Gatteschi, Phys. Rev. B **68**, 104403 (2003).
[23] R. Caciuffo, T. Guidi, G. Amoretti, S. Carretta, E. Liviotti, P. Santini, C. Mondelli, G. Timco, C. A. Muryn, and R. E. P. Winpenny, Phys. Rev. B **71**, 174407 (2005).
[24] J. Stohr, J. Electron Spectrosc. Relat. Phenom. **75**, 253 (1995).
[25] V. Bellini, A. Olivieri, and F. Manghi, Phys. Rev. B **73**, 184431 (2006).
[26] V. Bellini (private communication).
[27] M. A. Tomaz, W. J. Antel, Jr., W. L. O'Brien, and G. R. Harp, Phys. Rev. B **55**, 3716 (1997).
[28] E. Goering, A. Bayer, S. Gold, G. Schutz, M. Rabe, U. Rudiger, and G. Guntherodt, Phys. Rev. Lett. **88**, 207203 (2002).
[29] E. Gaudry, P. Sainctavit, F. Juillot, F. Bondioli, P. Ohresser, and I. Letard, Phys. Chem. Miner. **32**, 710 (2006).
[30] S. S. Dhesi, E. Dudzik, H. A. Durr, N. B. Brookes, and G. van der Laan, Surf. Sci. **454**, 930 (2000).
[31] C. Sorg, N. Ponpandian, A. Scherz, H. Wende, R. Nunthel, T. Gleitsmann, and K. Baberschke, Surf. Sci. **565**, 197 (2004).
[32] H. Wang, D. S. Patil, C. Y. Ralston, C. Bryant, and S. P. Cramer, J. Electron Spectrosc. Relat. Phenom. **114**, 865 (2001).
[33] G. van der Laan, B. T. Thole, G. A. Sawatzky, and M. Verdaguer, Phys. Rev. B **37**, 6587 (1988).
[34] G. van der Laan and B. T. Thole, Phys. Rev. B **43**, 13401 (1991).
[35] P. Carra, B. T. Thole, M. Altarelli, and X. Wang, Phys. Rev. Lett. **70**, 694 (1993).
[36] B. T. Thole, P. Carra, F. Sette, and G. van der Laan, Phys. Rev. Lett. **68**, 1943 (1992).
[37] J. Stohr and H. Konig, Phys. Rev. Lett. **75**, 3748 (1995).
[38] J. Stohr, J. Magn. Magn. Mater. **200**, 470 (1999), and references therein.
[39] C. T. Chen, Y. U. Idzerda, H. J. Lin, N. V. Smith, G. Meigs, E. Chaban, G. H. Ho, E. Pellegrin, and F. Sette, Phys. Rev. Lett. **75**, 152 (1995).
[40] Y. Teramura, A. Tanaka, and T. Jo, J. Phys. Soc. Jpn. **65**, 1053 (1996).